



**Universitat Autònoma  
de Barcelona**



**Facultat de Veterinària  
Departament de Ciència Animal i dels Aliments**

**Official Master's Degree in Food Quality of Animal Origin**

# **VALIDATION OF AN OPTICAL TECHNOLOGY FOR THE DETERMINATION OF pH IN MILK FOR THE MANUFACTURE OF YOGURT**

Special graduation project submitted for the overcoming of the 15 credits of the  
"Master's Thesis" Module as a requirement to qualify for the Master's Degree in  
Quality of Food of Animal Origin

Author: Siqi Liu  
Directors: Manuel Castillo Zambudio  
Oscar Arango Bedoya  
Bellaterra (Cerdanyola del Valles), September 2019

Declaro ser la autora de este Trabajo Fin de Máster que se presenta para obtener el grado de Maestría en Calidad de Alimentos de Origen Animal en la Universidad Autónoma de Barcelona, España. Este trabajo no ha sido presentado antes para obtener ningún grado o examen en cualquier otra universidad.

A handwritten signature in black ink, reading "Siqui Liu". The script is cursive and fluid, with the first name "Siqui" and the last name "Liu" clearly distinguishable.

Siqui Liu

Bellaterra, 3 de septiembre de 2019

Los Doctores Óscar Arango Bedoya (Facultad de Ingeniería Agroindustrial, Universidad de Nariño, Pasto, Colombia) y Manuel Castillo Zambudio (Área de Tecnología dels Aliments del Departament de Ciència Animal i dels Aliments de la Universitat Autònoma de Barcelona)

INFORMAN


Que el trabajo titulado: "Validación de una tecnología óptica de determinación del pH en leche para la elaboración de yogur" ha sido realizado, bajo su supervisión y tutela, por Siqi Liu durante la realización del Máster en Calidad de Alimentos de Origen Animal de la Universitat Autònoma de Barcelona.

Bellatera, septiembre de 2019

MANUEL  
CASTILLO  
ZAMBUDIO

Firmado digitalmente por  
MANUEL CASTILLO ZAMBUDIO  
Nombre de reconocimiento (DN):  
c=ES, ou=Vegeu <https://www.aoc.cat/CATCert/Regulacio>,  
sn=CASTILLO ZAMBUDIO,  
givenName=MANUEL,  
serialNumber=27485164A,  
cn=MANUEL CASTILLO ZAMBUDIO  
Fecha: 2019.09.03 17:16:16 +02'00'

Manuel Castillo Zambudio

  
Óscar Arango Bedoya  
Pasaporte ARO28612  
Colombia

## **ACKNOWLEDGEMENTS**

During the process of writing this final master's project, I have found many people who have played a crucial role. I am very happy to give my sincere thanks at the end of this work.

First of all, I want to thank my director Manuel Castillo Zambudio for giving me the opportunity to learn and research a new technology for producing yogurt. During this work, sometimes, I have not known how to move forward, but I have always received invaluable guidance from him. Every time when I have questions, he has patiently explained the theme to me and helped me to better understand it. He has also helped me a lot in experimental design and data analysis. I am very happy to have been able to have him as director and sincerely thank him for his patience and encouragement. Without his help, this work would not have been possible.

On the other hand, I also want to thank Oscar Arango Bedoya, my other director. Although we have never met in person, he has helped me a lot in my writing work, especially in the data analysis and discussion section, which has made this work a more significant and relevant one.

Beyond the academic environment, I thank the support of my family. Although my parents don't know Spanish or English, they always encourage and support me a lot. I would not have been able to come to Universitat Autònoma de Barcelona to study and improve my education without their help.

Finally, I am very grateful to all the professors of the Department of Animal and Food Science, my classmates and my friends, for your help and encouragement.

## CONTENTS

ACKNOWLEDGEMENTS.....	I
CONTENTS.....	II
ABSTRACT.....	III
RESUMEN .....	IV
RESUM.....	V
1 INTRODUCTION .....	1
2 MATERIALS AND METHODS .....	4
2.1 Experimental design.....	4
2.2 Preparation of milk.....	4
2.3 Preparation of starter culture .....	5
2.4 Acid milk coagulation induction .....	6
2.5 Measurement of the light backscatter ratio and pH.....	7
2.5.1 Determination of NIR light scatter parameters.....	7
2.5.2 Adjustment of the voltage gain.....	8
2.5.3 pH measurement .....	8
2.5.4 pH electrode calibration.....	9
2.5.5 Statistical Analysis.....	9
3 RESULTS AND DISCUSSION.....	11
3.1 Results of model without voltage gain adjustment ( <i>vat #2</i> ).....	14
3.1.1 Calibration and validation .....	14
3.1.2 Effects of temperature, protein and interaction between these two factors on the calibration coefficients.....	17
3.2 Results of model with voltage gain adjustment ( <i>vat #1</i> ).....	18
3.2.1 Calibration and validation .....	18
3.2.2 Effects of temperature, protein and interaction between these two factors on the calibration coefficients .....	21
3.3 Results of the external pH model with voltage gain adjustment ( $pH_E$ ).....	23
3.3.1 Calibration and validation .....	23
3.3.2 Effects of temperature, protein and interaction between these two factors on the calibration coefficients .....	25
CONCLUSIONS.....	29
REFERENCES .....	31

## **ABSTRACT**

Current systems that allow online pH control in fermented dairy industry have drawbacks, such as protein adhesion on the pH electrode and measurement distortion. Therefore, the objective of this experiment was to validate the feasibility of estimating the pH of milk during the yogurt making process by a NIR light backscatter sensor measuring at a wavelength of 880 nm under different fermentation temperatures and milk protein concentrations, using a mathematical model that correlates the light scatter signal with pH, developed by Arango (2005). Three replications of the experiment with 2 protein concentrations (3.5, and 4.0%), and 2 fermentation temperatures (43 and 46 °C) were used to validate this inline pH prediction model. Prior to the beginning of each treatment, different adjustments were made in the initial voltage gain in the two vats of the light scatter device to evaluate which of the two procedures allowed a better calibration of the pH prediction model. The results showed that the optical sensor was suitable for inline monitoring of yogurt acidification. Temperature and initial voltage were the main factors affecting the fitting accuracy of the model. More concretely, the model adjustment at 43 °C was better than at 46 °C, the adjustment of the initial voltage gain is recommended, and the model with voltage gain adjustment has been successfully validated for both continuous and discontinuous measurements of pH, with SEP values < 0.09 pH units and CV < 1.82%.

Keywords: yogurt fermentation, NIR light backscatter sensor, inline, monitoring, temperature, protein concentration.

## RESUMEN

Los sistemas actuales que permiten el control del pH en línea en la industria de fermentados lácticos tienen inconvenientes, como la adhesión de proteínas en el electrodo de pH y la distorsión de la medición. Por lo tanto, el objetivo de este experimento fue validar la viabilidad de estimación del pH de la leche durante el proceso de elaboración de yogur mediante un sensor de retrodispersión de luz NIR que mide a una longitud de onda de 880 nm, bajo diferentes temperaturas de fermentación y concentraciones de proteínas en leche, utilizando un modelo matemático que correlaciona la señal de dispersión de luz con el pH, desarrollado por Arango (2005). Se utilizaron tres repeticiones del experimento con 2 concentraciones de proteína (3,5 y 4,0%) y 2 temperaturas de fermentación (43 y 46 °C) para validar este modelo de predicción de pH en línea. Antes del comienzo de cada tratamiento, se realizaron diferentes ajustes en la ganancia de voltaje inicial en los procedimientos del dispositivo de dispersión de luz para evaluar cuál de los procedimientos permitía una mejor calibración del modelo de predicción de pH. Los resultados mostraron que el sensor óptico era adecuado para la monitorización en línea de la acidificación del yogur. La temperatura y el voltaje inicial fueron los principales factores que afectaron la precisión de ajuste del modelo. Más concretamente, el ajuste del modelo a 43 °C fue mejor que a 46 °C, se recomienda el ajuste de la ganancia de voltaje inicial y el modelo con ajuste de ganancia de voltaje fue validado con éxito tanto para mediciones continuas como discontinuas de pH, con valores de SEP < 0,09 unidades de pH y CV < 1,82%.

Palabras clave: fermentación de yogur, sensor de la dispersión de luz NIR, en línea, monitorización, temperatura, concentración de proteína.

## RESUM

Els sistemes actuals que permeten el control del pH en línia en la indústria de productes làctics fermentats tenen inconvenients, com l'adhesió de proteïnes en l'elèctrode de pH i la distorsió del mesurament. Per tant, l'objectiu d'aquest experiment va ser validar la viabilitat d'estimar el pH de la llet durant el procés d'elaboració de iogurt mitjançant un sensor de dispersió de llum NIR que mesura a una longitud d'ona de 880 nm. Es va utilitzar un model matemàtic, desenvolupat per Arango (2005), que correlaciona el senyal de dispersió de llum amb el pH, sota diferents temperatures de fermentació i concentracions de proteïnes de la llet. Es van dur a terme tres repeticions de l'experiment amb dues concentracions de proteïna (3,5 i 4,0%), i dues temperatures de fermentació (43 i 46 °C) per validar aquest model de predicció de pH en línia. Abans de començar cada tractament, es van realitzar diferents ajustos en el guany de voltatge inicial del dispositiu de dispersió de llum per avaluar quin dels procediments permetien un millor calibratge del model de predicció de pH. Els resultats van mostrar que el sensor òptic era adequat per al monitoratge en línia de l'acidificació del iogurt. La temperatura i el voltatge inicial van ser els principals factors que van afectar la precisió d'ajust del model. Més concretament, l'ajust del model a 43 °C va ser millor que a 46 °C i es recomana l'ajust del guany de voltatge inicial. El model amb ajust de guany de voltatge ha estat validat amb èxit tant per mesures contínues com discontinües de pH, amb valors de SEP < 0,09 unitats de pH i CV < 1,82%.

Paraules clau: fermentació de iogurt, sensor de dispersió de llum NIR, en línia, monitorització, temperatura, concentració de proteïna.

## 1 INTRODUCTION

Yogurt is one of the preferred dairy foods by consumers as a type of multi-functional food with high nutritional value, relatively low price, and long shelf-life. Currently, a large variety of yogurts are offered in the market, with different textures and flavors. It does not only retain the nutrients contained in milk, but also produce vitamins needed for human nutrition such as vitamins B<sub>6</sub> and B<sub>12</sub> during fermentation by lactic acid bacteria (LAB) (Liu, 2010). Furthermore, the fat content is relatively reduced in yogurt, especially in low-fat and non-fat yogurts. The Quality Standard for yogurt (RD 271/2014) stipulates that the fat content of semi-skimmed yogurts must be less than 2 and greater than 0.5%, and for skimmed yogurts it must be equal to or less than 0.5%. According to the survey of the National Institute of Statistics (INEbase, CPI, 2007), in Spain, yogurt consumption is 17 kg per person and year. Because of its huge market demand, the yogurt industrial production chain has matured, so the control of key points on the production line is required to be accurate, fast and efficient (Yu, 2004). Yogurt fermentation is the most important stage in yogurt manufacturing (Tamime and Robinson, 2007). At this stage, the inoculation, incubation and subsequent growth of LAB coagulates the milk and forms unique flavor characteristics, generating yogurt (Aswal et al., 2012).

The determination of the yogurt fermentation end-point (i.e., the end of the fermentation process) is essential for yogurt manufacturing. As a result of the high complexity of milk fermentation induced by lactic acid bacteria, an inadequate fermentation end-point selection could significantly compromise manufacturing cost and the final yogurt quality (Soukoulis et al., 2007). The casein micelle is sensitive to the change of pH value. Rasic and Kurmann's research (1978) showed that casein was completely precipitated at pH 4.7 - 4.6. Moreover, Spanish regulation establishes that all yogurts must have a pH equal to or less than 4.6 (RD 271/2014). Therefore, at industrial production, the yogurt fermentation process is controlled by pH.

To date, traditional electrochemical technology is used as the most common method for monitoring the fermentation process and determining pH of fermented dairy

products. This measurement method is usually carried out in a discontinuous manner, because continuous measurement can cause a series of problems such as protein adhesion on the pH electrode and measurement distortion (De Brabandere and De Baerdemaeker, 1999). At the same time, glass pH probes are at risk of rupture and therefore cannot be used for inline pH control at industrial scale.

For the above reasons, the traditional technology needs to collect samples manually every 10-15 min to measure the pH, which may result in contamination of the milk batch and poor real-time performance. As a result, pH control in yogurt fermentation greatly affects the production efficiency and increases the company's cost. As a response strategy to the risk of rupture of glass pH probes, an indestructible non-glass probe was developed, but the probe sensitivity of this material is lower than that of the glass electrode and is also affected by extreme conditions of pH and temperature during the in-situ cleaning operation (cleaning in place; CIP). Endress Hauser Group developed a pH sensor that can be retracted during CIP operation, which can be cleaned and calibrated automatically (Wesstrom, 2001). However, this system is complicated and costly; therefore, it is not a long-term solution in the preparation of industrial fermented dairy products.

Peris and Escuder (2013) gave an overview of some technologies that attempted to find new ways to monitor yogurt fermentation and determine its end-point. The lab-scale study of Cimander et al. (2002) fused signals from a NIR spectrophotometer, electronic nose and sensor data from the reactor temperature using a cascade neural network to monitor yogurt fermentation. Although the proposed technique achieved good results, there were some problems, such as the contamination of sensor elements, which may lead to calibration instability. In addition, the use of signals from a large number of sensors rises the cost of the technology being clearly impractical for inline application. Indeed, as indicated by Navrátil et al. (2004), the fusion of NIR and electronic nose has the potential to quickly monitor the quality of the fermentation process of yogurt and Filmjölkk (Swedish yogurt), under industrial conditions. However, the technique uses five or six PLS factors for prediction of pH and titratable acidity,

which undoubtedly increases the difficulty of model calibration and validation during the monitoring of yogurt fermentation; therefore, a large number of long-term studies is needed. In a PhD thesis by Arango (2015), a NIR light backscatter sensor was evaluated as an optic alternative method to pH probes, in order to monitor the yogurt fermentation process. The author used inulin as a fat substitute to study the yogurt fermentation process, gel formation and final firmness, and a model for inline prediction of pH value was successfully obtained.

In summary, in the fermented dairy products industry, the optimal incubation time is crucial. At the same time, the fermentation temperature and the protein content of the milk also affect the whole acid coagulation process, thus affecting both fermentation duration and quality of the yogurt. The traditional pH monitoring technology cannot control the pH continuously, accurately and conveniently. Therefore, this experiment refers to the method of Arango's research. The proposed optical technology, whose intellectual property belongs to the Universitat Autònoma de Barcelona (UAB) combines the use of a near infrared (NIR; 880 nm) light backscatter fiber optic sensor and a specific algorithm to convert, at real time, the sensor response into pH estimations. This technology can be operated inline, does not invade or destroy the sample, meets hygienic requirements, does not require continuous maintenance or pH calibration after installation, and it does not consume material or reagents. It avoids the drawbacks of traditional technology, can better determine the optimal incubation time, and complies with food regulations while reducing operating costs.

For this reason, the objective of the present investigation was to study the effect of temperature and protein concentration on the light scatter ratio response during acid coagulation using a NIR sensor, in order to calibrate and validate the yogurt pH prediction algorithms in the selected ranges of protein concentration and set temperatures.

## **2 MATERIALS AND METHODS**

### **2.1 Experimental design**

An experiment with three replications was designed and performed to study the effects of two different levels of incubation temperature (43 and 46 °C) and protein concentration (3.5 and 4.0%) on the yogurt fermentation process. This design had a total of 12 tests, which were performed randomly.

The light backscatter unit used in this experiment is equipped with two measuring vats prepared to continuously measure milk pH and light backscatter in parallel during coagulation. In order to evaluate if the effect of protein concentration and temperature on the initial voltage can be corrected and its effect on the pH prediction models used to improve the prediction algorithm performance, a correction on the initial voltage in one of the vats (vat #1) was made for each test, while in the other vat (vat #2), it was allowed to vary freely. The mentioned voltage correction will be explained in detail later.

In order to evaluate the pH progress in a similar manner to that used during industrial yogurt manufacturing, an aliquot of the inoculated milk was coagulated in a beaker inside a water bath at the same target temperature used in the light scatter unit, and samples were obtained every ~8 min to evaluate the pH progress using a regular external pH-meter. Then, continuous and discontinuous pH measurements were correlated to light scatter readings to pursue validation of the optical pH prediction method at different protein concentrations and fermentation temperatures.

### **2.2 Preparation of milk**

This experiment used commercial skimmed UHT milk purchased from a local supermarket in Spain as a raw material. What calls for special attention was that the whole experiment needed to use the same batch of milk for the purpose of minimizing the experiment variability associated to uncontrolled milk composition or pretreatment. The 1 L-bricks of milk were kept stored at 4 °C until opened and used. Milk sample was adjusted to the protein concentration required for each test using low-heat skim

milk powder (Chr. Hansen, Barcelona, Spain). The protein and fat composition of both skim UHT milk and skim milk powder is shown in table 1.

**Table 1.** Concentration of protein and fat in the raw materials used in the experiment.<sup>a</sup>

<b>Concentration</b>	<b>Skimmed UHT milk</b> <b>(g / 100 mL)</b>	<b>Skimmed milk powder</b> <b>(g / 100 g)</b>
<b>Protein (%)</b>	3.2	36.5
<b>Fat (%)</b>	0.3	0.9

<sup>a</sup>Information taken from the product label.

In this experiment, samples of ~500 mL, containing the target concentration of protein, according to the experimental design were prepared mixing skimmed UHT milk and skimmed milk powder. For each test, the sample was prepared as follows: 500 mL of skimmed UHT milk was measured in a volumetric flask, and the amount of milk powder required to achieve the target protein concentration was calculated and weighed in a beaker and added to the UHT milk. After this, the mixture was stirred with a magnetic stirrer for 30 min at 43 °C and then left to stand in the dark for another 30 min, protecting the sample from the air using parafilm. The sample was heated to 90 °C and left at this temperature for 5 min, after which it was quickly cooled to the target fermentation temperature, 43 °C or 46 °C, using an ice bath.

### 2.3 Preparation of starter culture

Considering the high content of live bacteria in the direct-vat-starter cultures (DVS), they are convenient and quick to use, simplifying the fermentation process. Furthermore, the use of this type of starter culture has a lower risk of phage infection during the fermentation process. This experiment used the commercial lyophilized culture of *Streptococcus thermophilus* and *Lactobacillus delbrueckii subsp. Bulgaricus* (YO-MIX 496 LYO 100 DCU, Danisco, Sassenage, France) as a starter culture for yogurt fermentation.

With the aim to maximize the activity of the inoculum, the commercial culture was first grown in skim milk. On the day of each test, 88 mL of skimmed milk powder, rehydrated to 12% total solids, was stirred and heat-treated at 90 °C for 5 min as described in point 2.2. Then, it was cooled to 43 °C, inoculated with 130 mg L<sup>-1</sup> DVS and the mixture was stirred and incubate at 43 °C until pH 5.0 was reached (Arango, 2015). This working culture was used as an inoculum for subsequent fermentation of the test milk sample at 2%.

## 2.4 Acid milk coagulation induction

For each test, the amount of the skimmed milk powder needed was calculated based on the protein content required for the experiment, and added to 500 mL of UHT milk as described in section 2.2. The protein adjusted mixture of UHT and milk powder was used for testing acid coagulation as shown in Fig. 1.

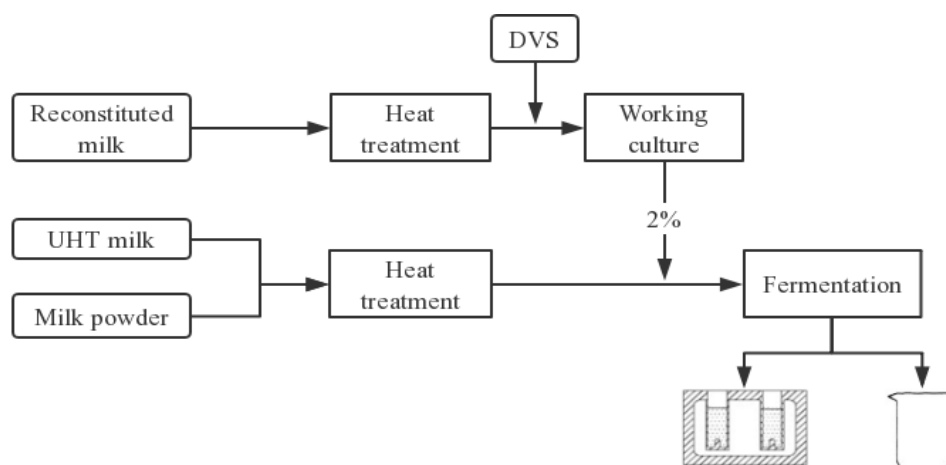


**Fig. 1.** Schematic diagram for comparing the traditional technique for yoghurt fermentation end-point selection with the alternative optical end-point selection method using near infrared light backscatter.

The temperature control system was previously set at its required incubation temperature (43 °C or 46 °C). Then the mixture was left in a thermostatic bath at the corresponding incubation temperature until thermal equilibrium was reached. At that time, 10 g (2%) of working culture prepared as described in section 2.3 was added and

the whole liquid was stirred with a spatula for 1 min. Two aliquots of 80 mL were poured into the two vats of the optical unit, which will be described in section 2.5.1. At each vat, pH electrodes were placed through a hole located in the lid of the vat. Data acquisition corresponding to both light backscatter sensors and pH electrodes (vats #1 and #2) were immediately initiated at the time of inoculum addition. The remaining sample (340 mL) was placed in a sealable beaker and sampled every 8 min to measure the pH, using a standard pH meter connected to a glass pH electrode.

## 2.5 Measurement of the light backscatter ratio and pH

### 2.5.1 Determination of NIR light scatter parameters

The optical apparatus used to determine near infrared light backscatter at 880 nm during milk coagulation named CoAguLab, was designed at the University of Kentucky. Its design was described in detail in the paper of Tabayehnejad et al. (2012). A brief description follows. It has two vats that simultaneously monitor the acid coagulation of two samples for accurate comparison (Fig. 2). An optic unit directs near infrared light from an LED emitting at 880 nm to the milk sample through an optical fiber while a second fiber returns backscattered light at 180 degrees back to a silicon detector.

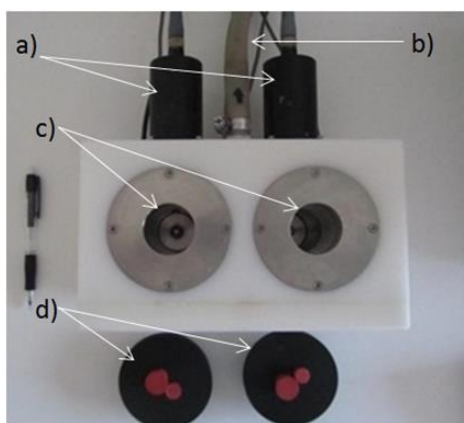


**Fig.2.** Top view of the CoAguLab unit showing: a) optical sensors, b) water outlet for temperature control (the water inlet is below), c) stainless steel vats where the samples are deposited, d) plastic caps to prevent surface evaporation, with access to insert pH electrodes.

\*Reproduced from Arango (2015).

The scattered light is linearly converted by the sensor into a voltage signal. The voltage is measured every two seconds and the average of three measurements is recorded every six seconds. The equipment is zeroed switching off the led and adjusting the voltage reading to zero volts. Once milk coagulation monitoring is initiated, the first ten voltage registers are averaged to calculate the initial voltage ( $V_0$ ). Once  $V_0$  is calculated, the light backscatter ratio ( $R$ ) is obtained by dividing the voltage measured every six seconds by  $V_0$ .

### 2.5.2 Adjustment of the voltage gain

To evaluate if the effect of protein concentration and temperature on the initial voltage could be corrected, the following procedure was carried out: before starting data acquisition, the voltage of vat #1 was adjusted to 2.00 V, using the sample prepared for each test, when the treatment temperature was in equilibrium. Contrarily, for vat #2, the voltage was only adjusted to 2.00 V before the first treatment of each replication; and then it was let to vary freely according to coagulation temperature and protein concentration in each test.

### 2.5.3 pH measurement

Development of the proposed optical pH prediction model was done based on continuous and simultaneous acquisition of both pH and light backscatter measurements during acid coagulation, as a function of time. However, yogurt fermentation end-point is selected worldwide sampling yogurt every 10-15 min up to pH 4.6 is reached. As a result, two pH measurement procedures were used in the study. On one hand, the pH on each vat (#1 and #2) was measured using separate pH electrodes placed on the milk of the vat through a hole on the lid of each vat. The electrodes (Thermo Scientific™ Orion 8104BN ROSS, Switzerland) were connected to the data acquisition enclosure of the CoAguLab tester. These pH measurements were collected every 6 s. On the other hand, the milk sample that was fermented inside the external

water bath, in parallel to those samples placed in vats #1 and #2, was sampled manually. Every 8 min, a small aliquot was collected and placed in a small beaker. The sample was stirred and the pH was measured using an external pH electrode (Model 50 12T, Crison Instruments, S. A., Spain) connected to a pH-meter (Model pH BASIC 20, Crison Instrument). As the discontinuous pH data was taken every 8 min, the external pH curves were adjusted as a function of time, by polynomial expressions in order to estimate pH data every 6 seconds. This procedure allowed to expand the number of datapoints for calibration.

#### 2.5.4 pH electrode calibration

Prior to each test, the electrodes attached to the CoAguLab system and the one connected to the external pH-meter were calibrated separately using the standard buffer solutions of pH = 7.00 and pH = 4.01 at the corresponding tested temperatures. After calibration was complete, pH electrodes were stored in the storage solutions recommended by the manufacturers. While electrodes connected to the CoAguLab unit were stored using storage solution Cat. No. 810001, the external electrode used storage solution CRISOLYT-A (KCl 3M + AgCl). When each replication was completed, all the electrodes were cleaned, following the manufacturer cleaning protocol and the recommended cleaning solution, to prevent protein precipitation and salt deposits.

#### 2.5.5 Statistical Analysis

A prediction model that transforms the light backscatter ratio measured by the acid coagulation tester into real time pH measurements [ $\text{pH} = f(R)$ ], proposed by Arango (2015) was calibrated and validated in this study. As established by this author, the row data corresponding to the pH values in the range of 5.2–4.6 were selected as the “working” data set for statistical analysis. Two of the three replications were used for calibration of the model. Three possible two-replication combinations were tested for calibration: replications one-two, one-three and two-three, while the replication not

employed for calibration in each of the three cases was utilized for validation. Calibration of the model was performed using CurveExpert software (CurveExpert Professional version 2.6.5, Daniel G. Hyams, Huntsville, USA), which allowed to estimate the four different regression coefficients contained in the prediction model ( $\beta_1$ ,  $\beta_2$ ,  $\beta_3$ , and  $\beta_4$ ; coded randomly with numbers between 1 and 4 for confidentiality reasons). The regression coefficients obtained were processed using SAS software (SAS version 2009, SAS Institute Inc., Cary, NC, USA) and analyzed by analysis of variance (ANOVA) using the general linear model GLM. The main factors included in the statistical model were the replication (*Rep*), protein concentration (P) and fermentation temperature (T) evaluated in this experiment, as well as the interaction between these three factors (T x P; T x *Rep*; P x *Rep*). A preliminary ANOVA analysis was run to evaluate the significance of each factor. Only significant factors were included in the final ANOVA analysis. The least squares mean (LS-MEANS) and the significance of each treatment were calculated using the sum of squares of Type IV. When  $P < 0.05$ , differences between treatment means were considered to be significant. In addition, different adjustments of the initial voltage were made, as was explained in detail in section 2.5.2, in order to evaluate statistically which of the two procedures allows a better adjustment of the pH prediction model.

### 3 RESULTS AND DISCUSSION

In this study, lactic acid fermentation was carried out under different gelation temperatures and protein concentrations conditions. The relationship between the light backscatter ratio (R), the pH profiles and the first derivative of R as a function of time is shown in Figs. 3 and 4. Since the curves obtained under the same protein concentration and temperature for each of the three replications were approximately the same, the data of Figs. 3 and 4 was selected from the replica 2.

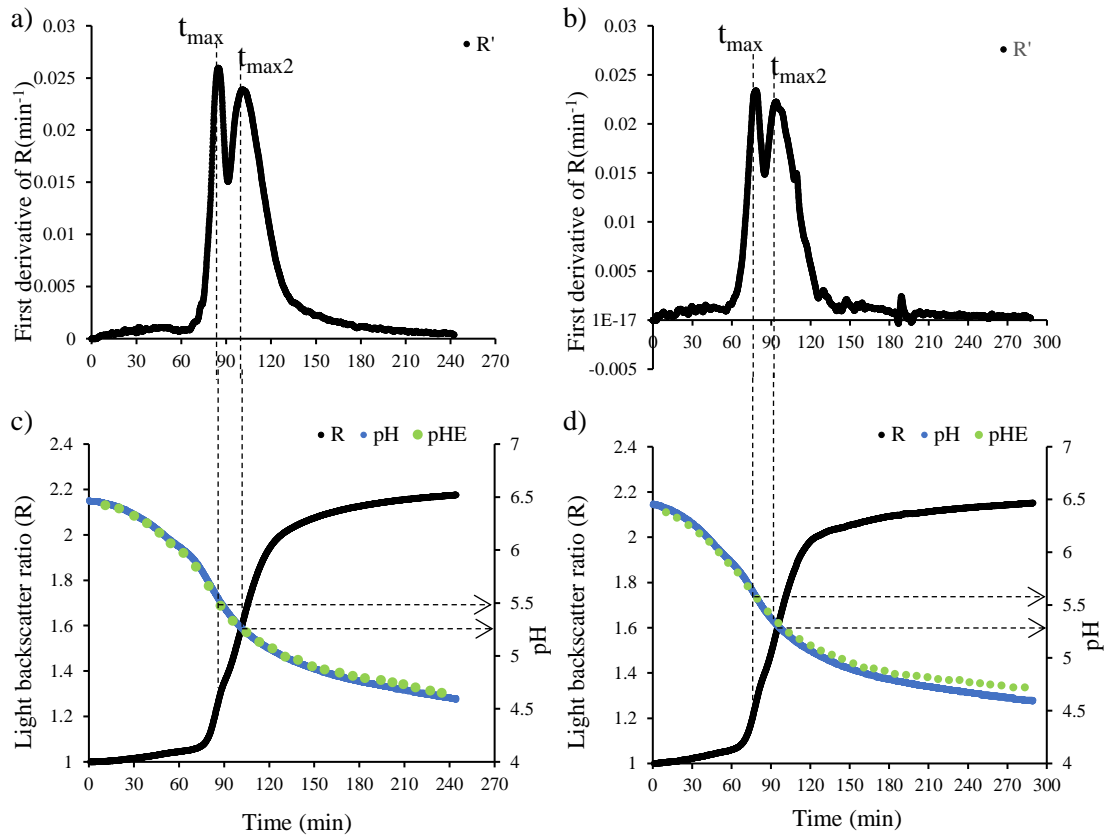


**Fig. 3.** The relationship between the light backscatter ratio and pH profiles with 3.5% protein concentration at c) 43 °C and d) 46 °C. The first derivative of R versus time at a) 43 °C and b) 46 °C. Data correspond to vat #1 of replica 2. R, light backscatter ratio; pH, pH value measured by CoAguLab; pHE, discontinuous, external pH measurements. R', first derivative of R( $\text{min}^{-1}$ );  $t_{max}$ , first maximum of the first derivative;  $t_{max2}$ , second maximum of the first derivative.

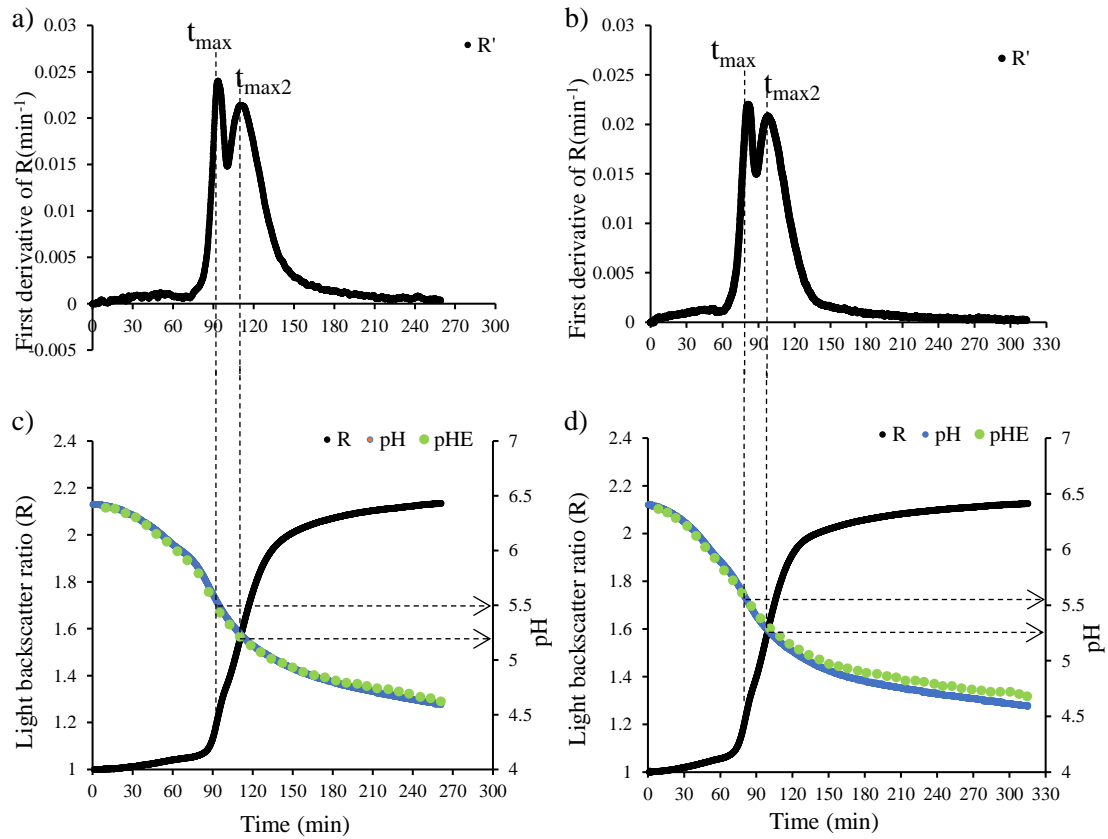


**Fig. 4.** The relationship between the light backscatter ratio and pH profiles with 4.0% protein concentration at c) 43 °C and d) 46 °C. The first derivative of R versus time at a) 43 °C and b) 46 °C. Data correspond to vat #1 of replica 2. R, light backscatter ratio; pH, pH value measured by CoAguLab; pH<sub>E</sub>, discontinuous, external pH measurements; R', first derivative of R(min<sup>-1</sup>);  $t_{max}$ , first maximum of the first derivative;  $t_{max2}$ , second maximum of the first derivative.

As indicated by Figs. 3 and 4, milk pH before yogurt fermentation was ~6.5 - 6.4. Bacterial growth initiated a slow decrease of pH induced by lactic acid production from lactose. The coagulation of yogurt happened in two stages, and the first stage was defined by calculating the  $t_{max}$  value obtained by the first derivative of R vs time (Fig. 3a, 3b, 4a, 4b). The decline of pH was at about maximum rate when pH reached a value of ~5.7-5.5, corresponding to  $t_{max}$ , where a first aggregation occurred due to the denatured particles of the serum proteins that bind to each other and with the casein micelles. This was consistent with the results of both Arango (2015) and Lee and Lucey (2004). Then, there was a second stage, which was identified by the second maximum

of R ( $t_{\max 2}$ ). During the fermentation process, the decrease of milk pH caused the colloidal calcium phosphate (CCP) within casein micelles to solubilize. This process is typically completed when the pH is  $\sim 5.0$ , if most whey proteins remain native (Lucey, 2002). At this point, the milk pH is close to the isoelectric point of casein (IP  $\sim 4.6$ ), which helps to enhance the attraction between the casein and thus increases the gel hardness (Lucey, 2002; Lee and Lucey, 2004). However, applying an intense heat treatment to milk, prior to fermentation, denatures a significant amount of whey proteins, which attach to casein micelles surface, inducing an IP shift, as a result of the higher isoelectric pH of whey proteins (Lucey, 1997a). Thus, due to the heat treatment of milk applied in this experiment ( $90\text{ }^{\circ}\text{C}$  during 5 min), denaturation of whey proteins modified the IP of the gel system at which gelatinization occurred. Based on the second maximum of the first derivative of Figs. 3a, 3b, 4a and 4b, the beginning of the second stage of milk fermentation, aggregation of demineralized and destabilized micelles, took place at a pH  $\sim 5.2$ . From that moment the gel hardening continues as the pH continues to decrease.

Figs. 3a and 4a showed the first derivative curve ( $R'$ ) of R with different protein concentrations at  $43\text{ }^{\circ}\text{C}$  while, similarly, Figs. 3b and 4b showed the first derivative curve of R at  $46\text{ }^{\circ}\text{C}$ . Comparing Fig. 3a with 3.5% protein concentration and Fig. 4a with 4.0% protein concentration (both at  $43\text{ }^{\circ}\text{C}$ ), it was found that different protein concentrations had no effect on the values of  $t_{\max}$  and  $t_{\max 2}$ . Similar behavior was observed for the effect of protein at  $46\text{ }^{\circ}\text{C}$  (Figs. 3b and 4b). Conversely, Figs. 4a and 4b (4.0% protein but different temperature) showed that temperature may affect the rate of coagulation, which was expected.

When the concentration of protein remained unchanged at 4.0%, the first stage of aggregation was relatively late at  $43\text{ }^{\circ}\text{C}$  (Fig. 4a), at which time the value of  $t_{\max}$  was 93.2 min; and when the temperature was raised from  $43\text{ }^{\circ}\text{C}$  to  $46\text{ }^{\circ}\text{C}$ , microbial metabolism and physicochemical reactions were more accelerated, which made the aggregation of the first stage of fermentation quicker, and  $t_{\max}$  advanced to 81.4 min (Fig. 4b). Similarly, the onset of coagulation and hardening, demarcated by  $t_{\max 2}$ , may

be anticipated with the increase in temperature. Comparing Figs. 4a and 4b, at the same protein concentration (4.0 %), the value of  $t_{\max 2}$  corresponding to 43 °C was 110.4 min, while when the fermentation temperature raised to 46 °C,  $t_{\max 2}$  was 12.7 min shorter (97.7 min). Similar behavior as a function of temperature was observed for  $t_{\max}$  and  $t_{\max 2}$  at 3.5% protein (Figs. 3a and 3b).

Various studies have shown that increasing the fermentation temperature increased whey separation, which was the same as the experimental phenomenon observed in this experiment, that was, the yogurt fermented at 46 °C produced more whey (not measured but observed). The paper of Lucey (2001) and Melema et al. (2002) demonstrated that high incubation temperature made the gel network more unstable and were more prone to protein network rearrangement, resulting in greater whey separation.

The experimental results corresponding to calibration and validation of the optical pH prediction model (Arango, 2015) for the three different pH acquisition systems evaluated were analyzed separately and are presented below.

### **3.1 Results of model without voltage gain adjustment (*vat* #2)**

#### **3.1.1 Calibration and validation**

Calibration and validation of the pH prediction model was performed using experimental data corresponding to each temperature and protein concentration combination, according to the method described previously (section 2.5.5). The resulting coefficients of determination ( $R^2$ ), standard errors of prediction (SEP), and coefficients of variation (CV) for model calibration as well as validation were used as model performance indicators, and are shown in Table 2.

It was evident from Table 2 that model calibration and validation were greatly affected by temperature. For protein concentration of 3.5%, the  $R^2_v$ ,  $SEP_v$ , and  $CV_v$  values at 43 °C were  $0.989 \pm 0.003$ ,  $0.46 \pm 0.24$ , and  $0.965 \pm 0.504$ , respectively while rising fermentation temperature to 46 °C yielded smaller  $R^2_v$ , and larger  $SEP_v$ , and  $CV_v$  values ( $0.771 \pm 0.147$ ,  $0.116 \pm 0.048$ ,  $2.400 \pm 0.949$ , respectively). The accuracy of the pH prediction model is indicted by high value of  $R^2$ , and small values of both SEP and

CV (Kawasaki et al., 2008). The observed effect of fermentation temperature on model calibration and validation for protein concentration of 4.0% was quite similar to that of 3.5% protein. So as the temperature rised, the results showed that the fitting accuracy was lower. On the other hand, it was observed that increasing the protein concentration worsened the adjustment, although the result is less clear than the effect of increasing the temperature. At 43 °C, increasing the protein concentration from 3.5% to 4.0% decreased the fitting accuracy ( $R^2_v$  from  $0.989 \pm 0.003$  to  $0.833 \pm 0.133$ ;  $SEP_v$  from  $0.046 \pm 0.024$  to  $0.085 \pm 0.036$ ;  $CV_v$  from  $0.965 \pm 0.504$  to  $1.769 \pm 0.728$ ), the same result was observed at 46 °C.

**Table 2.** Model performance indicators obtained at different temperature and protein concentration levels (vat #2).

Treatments		A		B		C		D		Average $\pm$ SD
Parameters		T (°C)	P (%)	T (°C)	P (%)	T (°C)	P (%)	T (°C)	P (%)	
		43	3.5	43	4.0	46	3.5	46	4.0	
Calibration	$R^2_c$	$0.972 \pm 0.023$		$0.855 \pm 0.089$		$0.748 \pm 0.185$		$0.792 \pm 0.097$		$0.792 \pm 0.097$
	$SEP_c$	$0.024 \pm 0.014$		$0.054 \pm 0.015$		$0.065 \pm 0.022$		$0.062 \pm 0.012$		$0.051 \pm 0.016$
	$CV_c$	$0.493 \pm 0.297$		$1.126 \pm 0.321$		$1.365 \pm 0.455$		$1.300 \pm 0.244$		$1.071 \pm 0.329$
Validation	$R^2_v$	$0.989 \pm 0.003$		$0.833 \pm 0.133$		$0.771 \pm 0.147$		$0.715 \pm 0.258$		$0.827 \pm 0.135$
	$SEP_v$	$0.046 \pm 0.024$		$0.085 \pm 0.036$		$0.116 \pm 0.048$		$0.107 \pm 0.054$		$0.089 \pm 0.040$
	$CV_v$	$0.965 \pm 0.504$		$1.769 \pm 0.728$		$2.400 \pm 0.949$		$2.267 \pm 1.191$		$1.850 \pm 0.843$

For treatment combinations A, B, C and D, data were means  $\pm$  standard deviations of three replications.  $R^2_c$ , coefficient of determination of calibration;  $R^2_v$ , coefficient of determination of validation;  $SEP_c$ , standard error of prediction of calibration (pH units);  $SEP_v$ , standard error of prediction of validation (pH units);  $CV_c$ , coefficient of variation of calibration (%);  $CV_v$ , coefficient of variation of validation (%). N, number of experiments, N = 12.  $N_c$ , total number of calibration datapoints,  $N_c$  = 3450.  $N_v$ , total number of validation datapoints,  $N_v$  = 1725.

Moreover, from the results in Table 2, the average value of  $R^2_v$  was only  $0.827 \pm 0.135$  well below the value corresponding to treatment combination A (3.5% protein and 43 °C;  $R^2_v = 0.989 \pm 0.003$ ). Thus with unadjusted voltage gain, increasing protein

and temperature levels may affect the accuracy of the prediction models.

The relationship between the predicted and observed pH values is shown in Fig. 5.

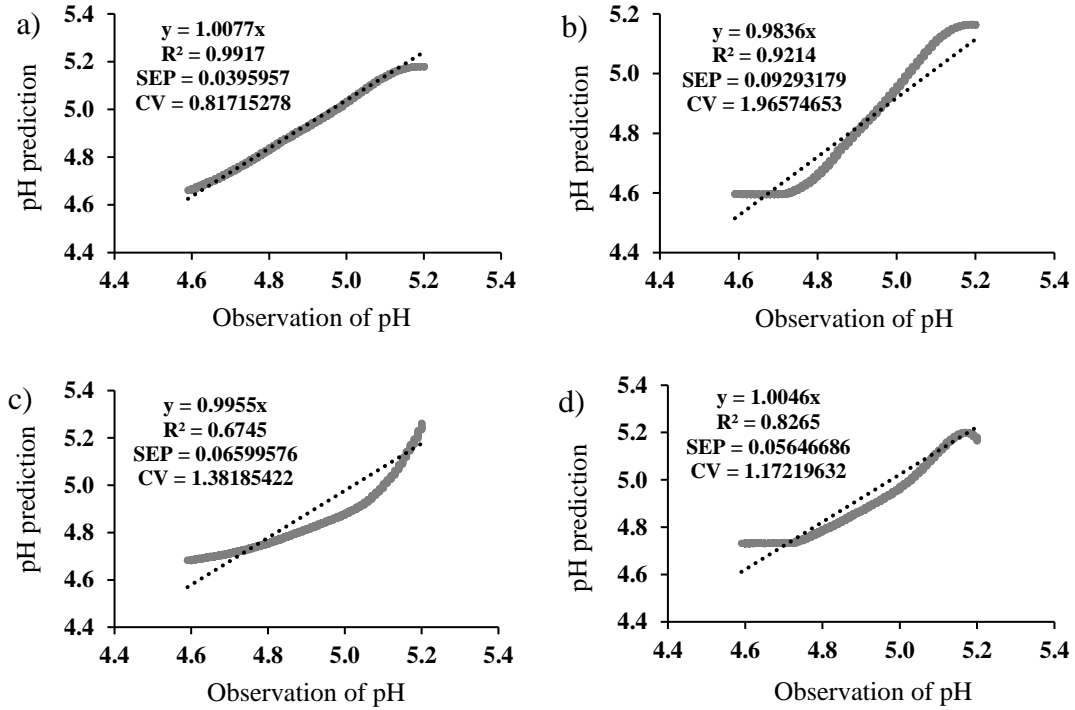


**Fig. 5.** Validation of the pH prediction model, without initial voltage gain adjustment. Validation data correspond to replication 3. N, number of validation datapoints;  $R^2$ , coefficient of determination; SEP, standard error of prediction (pH units); CV, coefficient of variation (%); a) data at 43 °C and 3.5% of protein, N = 1366; b) data at 43 °C and 4.0% of protein, N = 1516; c) data at 46 °C and 3.5% of protein, N = 2067; d) data at 46 °C and 4.0% of protein, N = 2032.

Based on Fig. 5, it should be highlighted that in all four evaluated conditions, SEP was  $< 0.094$  pH units, with CV  $< 2\%$ . However, it was evident by the distribution of the residuals along the pH scale, that only the results at 3.5% protein concentration and 43 °C were in line with expectations (Fig. 5a). This results suggested that absence of initial voltage gain adjustment seems to negatively affect the accuracy of the pH prediction model.

### 3.1.2 Effects of temperature, protein and interaction between these two factors on the calibration coefficients.

After preliminary analysis of the experimental data by ANOVA, it was concluded that there was no significant data variability attributable to *Rep*, *Rep* x *T*, *Rep* x *P* and *T* x *P*. Therefore, after eliminating the above listed effects and interactions, the influence of the main experimental factors (*T* and *P*) on the calibration regression coefficients were studied as shown in Figs. 6 and 7.

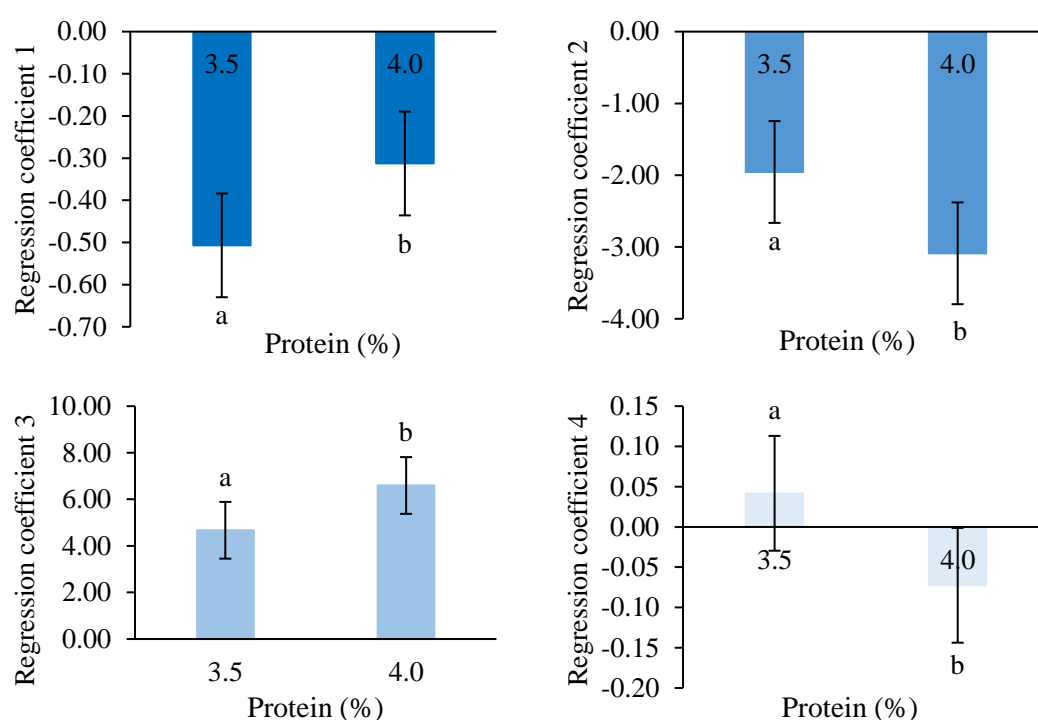


**Fig. 6.** Effect of different protein concentration on the calibration coefficients (1, 2, 3, 4) of the pH prediction model, without adjusting initial voltage gain. The error bars represented the standard deviation, N = 12. Least squares means (LSM) with different letters within the same subfigure are significantly different ( $p < 0.01$ ).

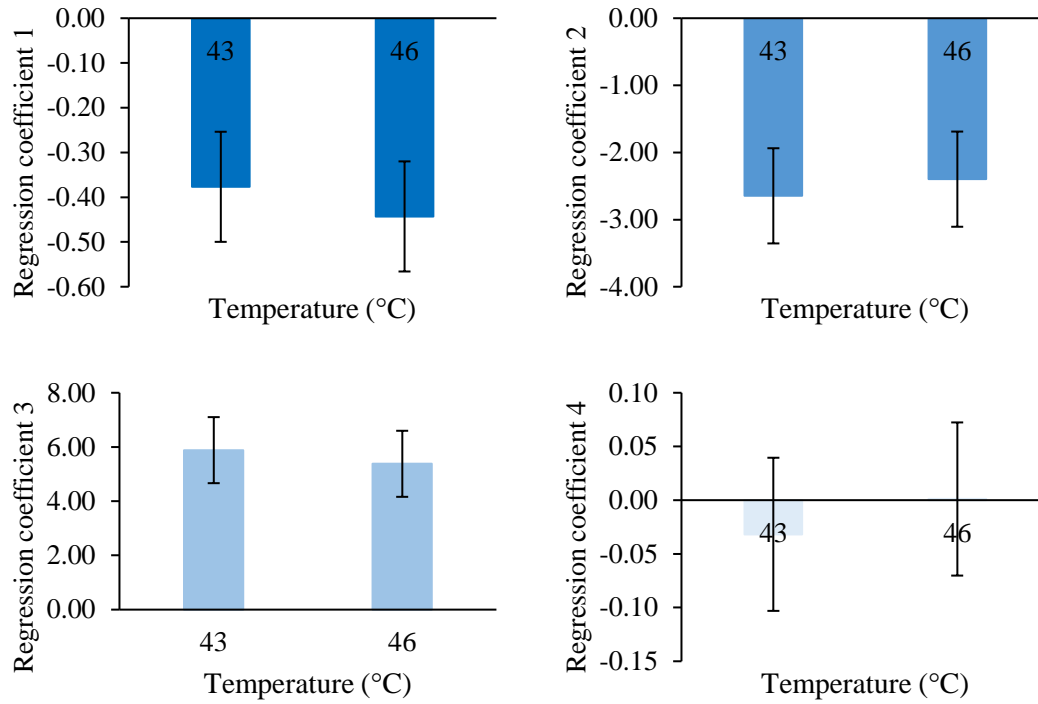


**Fig. 7.** Effect of different incubation temperature on the calibration coefficients (1, 2, 3, 4) of the pH prediction model, without adjusting initial voltage gain. The error bars represented the standard deviation, N = 12. Least squares means (LSM) without letters indicates no significantly different ( $p \geq 0.05$ ).

According to the ANOVA, no significant interactions were detected and temperature did not significantly affect any of the four regression coefficients ( $p \geq 0.05$ ). Only protein concentration affected significantly ( $p < 0.01$ ) the calibration coefficients. The effect of protein in the regression coefficients should allow improving the prediction models in future stages of this research.

### 3.2 Results of model with voltage gain adjustment (*vat #1*)

#### 3.2.1 Calibration and validation

Similarly to methodology described in section 3.1.1, model calibration and validation were performed on the data obtained at the same protein concentration and temperature and the results corresponding to model performance indicators is shown in Table 3.

**Table 3.** Model performance indicators obtained at different temperature and protein concentration levels (vat #1).

Treatments		A		B		C		D		Average $\pm$ SD
Parameters		T (°C)	P (%)	T (°C)	P (%)	T (°C)	P (%)	T (°C)	P (%)	
		43	3.5	43	4.0	46	3.5	46	4.0	
Calibration	$R^2_c$	0.998 $\pm$ 0.001		0.988 $\pm$ 0.009		0.877 $\pm$ 0.099		0.916 $\pm$ 0.062		0.945 $\pm$ 0.043
	SEP <sub>c</sub>	0.008 $\pm$ 0.002		0.017 $\pm$ 0.007		0.048 $\pm$ 0.022		0.041 $\pm$ 0.014		0.028 $\pm$ 0.011
	CV <sub>c</sub>	0.166 $\pm$ 0.039		0.344 $\pm$ 0.153		0.994 $\pm$ 0.457		0.860 $\pm$ 0.291		0.591 $\pm$ 0.235
Validation	$R^2_v$	0.998 $\pm$ 0.001		0.994 $\pm$ 0.005		0.932 $\pm$ 0.023		0.943 $\pm$ 0.039		0.967 $\pm$ 0.017
	SEP <sub>v</sub>	0.012 $\pm$ 0.005		0.030 $\pm$ 0.012		0.086 $\pm$ 0.042		0.070 $\pm$ 0.036		0.049 $\pm$ 0.023
	CV <sub>v</sub>	0.240 $\pm$ 0.094		0.617 $\pm$ 0.248		1.775 $\pm$ 0.834		1.454 $\pm$ 0.755		1.021 $\pm$ 0.483

For treatment combinations A, B, C and D, data were means  $\pm$  standard deviations of three replications.  $R^2_c$ , coefficient of determination of calibration;  $R^2_v$ , coefficient of determination of validation; SEP<sub>c</sub>, standard error of prediction of calibration (pH units); SEP<sub>v</sub>, standard error of prediction of validation (pH units); CV<sub>c</sub>, coefficient of variation of calibration (%); CV<sub>v</sub>, coefficient of variation of validation (%). N, number of experiments, N = 12. N<sub>c</sub>, total number of calibration datapoints, N<sub>c</sub> = 3396. N<sub>v</sub>, total number of validation datapoints, N<sub>v</sub> = 1698.

According to the results shown in Tables 2 and 3, the model with adjusted initial voltage gain yielded better predictions than those of vat #2 (without adjustment). According to the inference of section 3.1.1, when protein remained the same, the higher the temperature, the lower the fitting accuracy of the prediction model. Similarly, with adjusted voltage gain, when the protein concentration was 3.5%, the accuracy of prediction model reduced with temperature, increasing from 43 °C to 46 °C ( $R^2_v$  from 0.998  $\pm$  0.001 to 0.932  $\pm$  0.023; SEP<sub>v</sub> from 0.012  $\pm$  0.005 to 0.086  $\pm$  0.042; CV<sub>v</sub> from 0.240  $\pm$  0.094 to 1.775  $\pm$  0.834). This same effect also applied to 4.0% protein concentration. On the other hand, similar values of  $R^2_v$  and SEP<sub>v</sub> were obtained depending on protein at 43 °C (0.998  $\pm$  0.001 and 0.994  $\pm$  0.005, 0.012  $\pm$  0.005 and 0.030  $\pm$  0.012 for 3.5% and 4.0%, respectively). This result also happened at 46 °C. The best  $R^2_v$ , SEP<sub>v</sub> and CV<sub>v</sub> values of validation were obtained at a combination of

43 °C and 3.5% protein concentration, which were  $0.998 \pm 0.001$ ,  $0.012 \pm 0.005$  and  $0.240 \pm 0.094$ , respectively.

In order to show the data of Table 2 more intuitively, the replication 2 with the highest predicted pH accuracy in the model was selected, and the relationship between pH predicted value and true value is shown in Fig. 8.

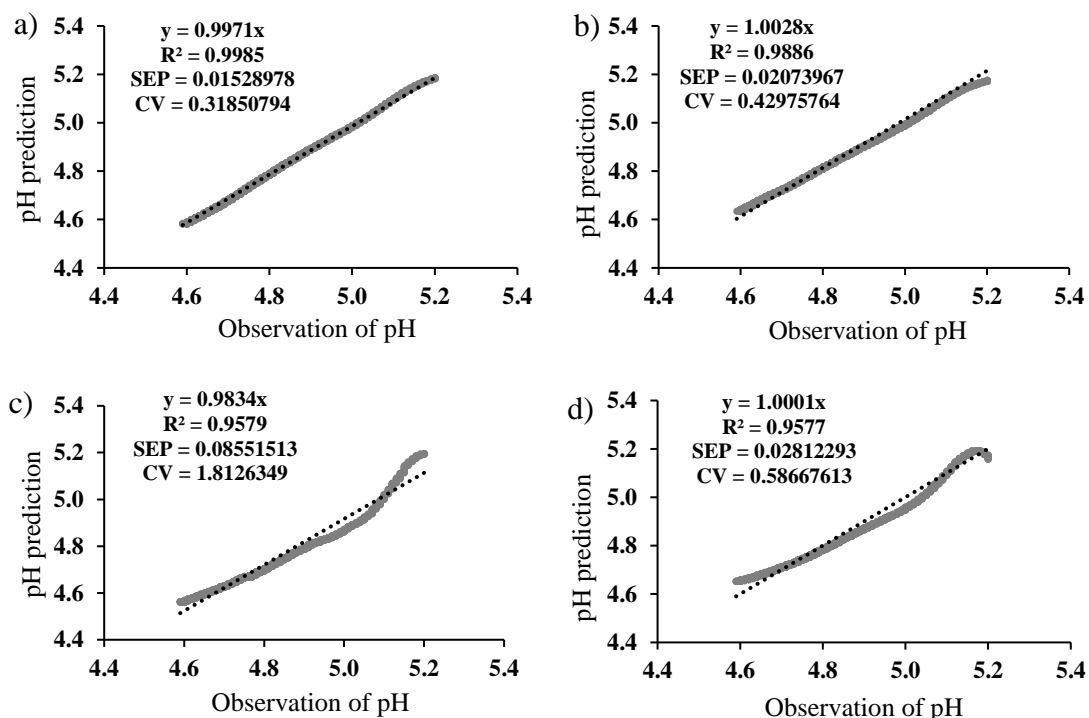


**Fig. 8.** Validation of the pH prediction model, with adjusted initial voltage gain. Validation data correspond to replication 2. N, number of validation datapoints;  $R^2$ , coefficient of determination; SEP, standard error of prediction (pH units); CV, coefficient of variation (%). a) data at 43 °C and 3.5% of protein. N = 1382; b) data at 43 °C and 4.0% of protein. N = 1480; c) data at 46 °C and 3.5% of protein. N = 1856; d) data at 46 °C and 4.0% of protein. N = 2095.

From Figs. 8a and 8b, it was evident that the coincidence degree of pH predicted and true values was quite high, especially at 43 °C. Although the accuracy of Figs. 8c and 8d was not completely satisfying, the predictions were better than the results of Figs. 5c and 5d from vat #2.

### 3.2.2 Effects of temperature, protein and interaction between these two factors on the calibration coefficients

The results of the preliminary analysis of ANOVA screened out the effects of all factors associated with the *Rep* on the calibration coefficients, such as *Rep*, *Rep* x *T*, *Rep* x *P*.

The effect of *T*, *P* and *T* x *P* on the calibration coefficients yielded from the secondary analysis is shown in Figs. 9, 10 and 11.

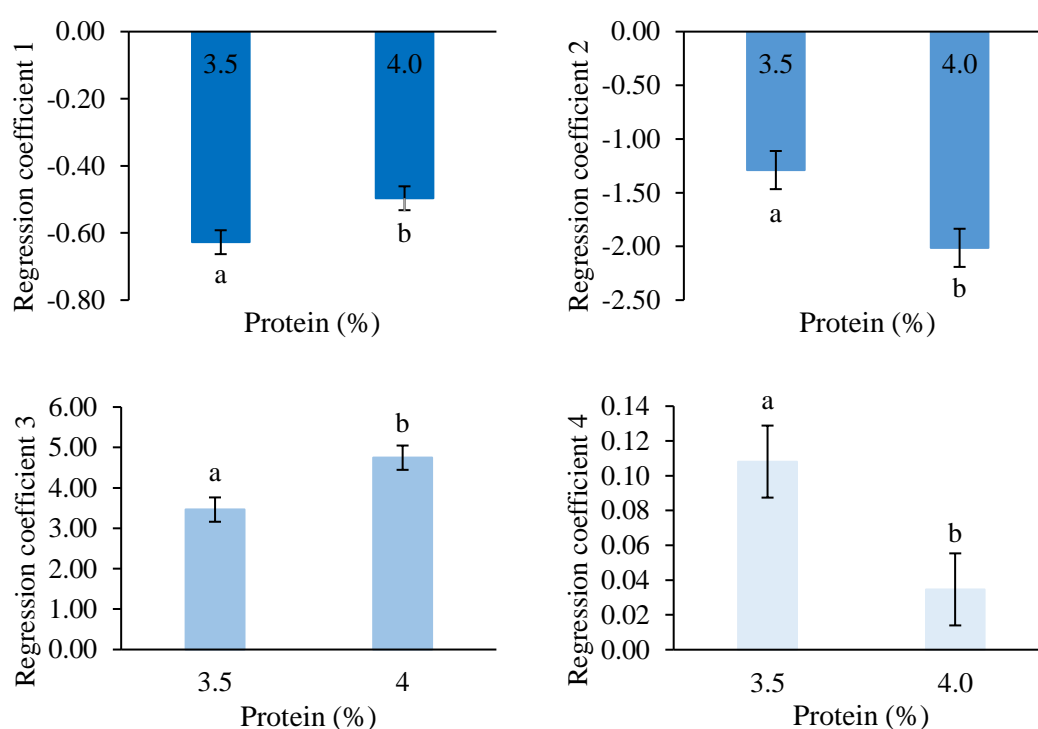


**Fig. 9.** Effect of different protein concentration on the calibration coefficients (1, 2, 3, 4) of the pH prediction model, with adjusted initial voltage gain. The error bars represented the standard deviation,  $N = 12$ . Least squares means (LSM) with different letters within the same subfigure are significantly different ( $p < 0.001$ ).

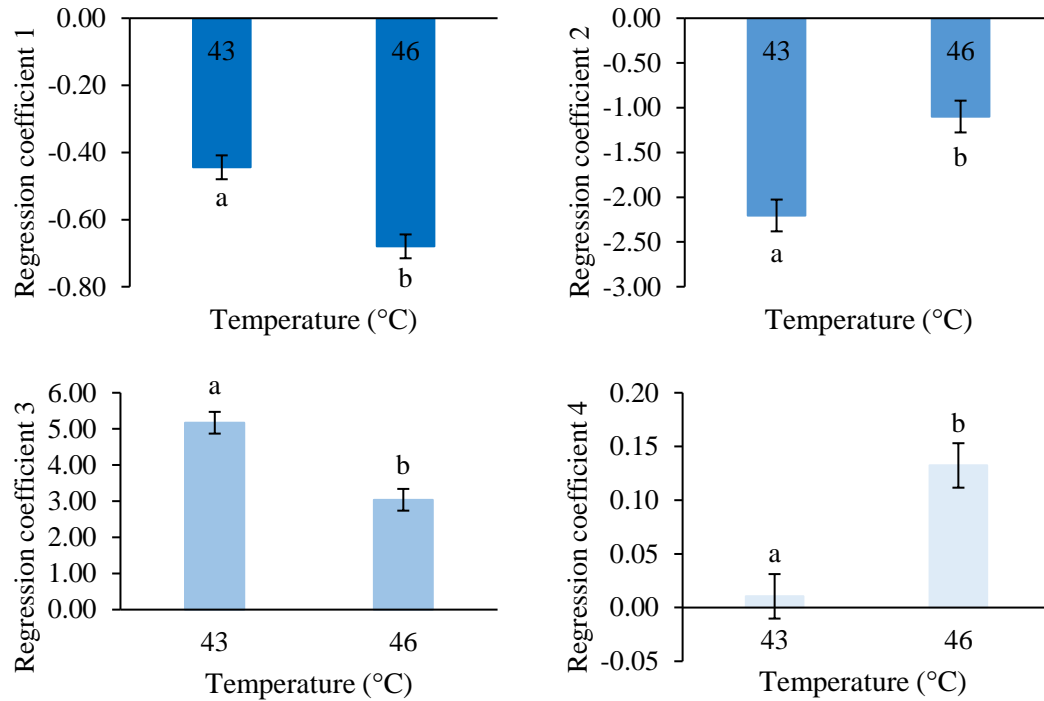


**Fig. 10.** Effect of different incubation temperature of the yogurt fermentation on the calibration coefficients (1, 2, 3, 4) of the pH prediction model, with adjusted initial voltage gain. The error bars represented the standard deviation, N = 12. Least squares means (LSM) with different letters within the same subfigure are significantly different ( $p < 0.001$ ).

Observing Figs. 9 and 10, for the model with adjusted initial voltage gain, both fermentation temperature and protein concentration affected each of the calibration coefficients ( $p < 0.001$ ). As can be seen in Fig. 11, the interaction of T x P was also statistically significant. Furthermore, since the slope is always higher with 3.5% protein concentration than with 4.0% protein, it is observed that the effect of temperature on the calibration coefficients (1, 2, 3, 4) is greater at 3.5% protein concentration than 4.0%.

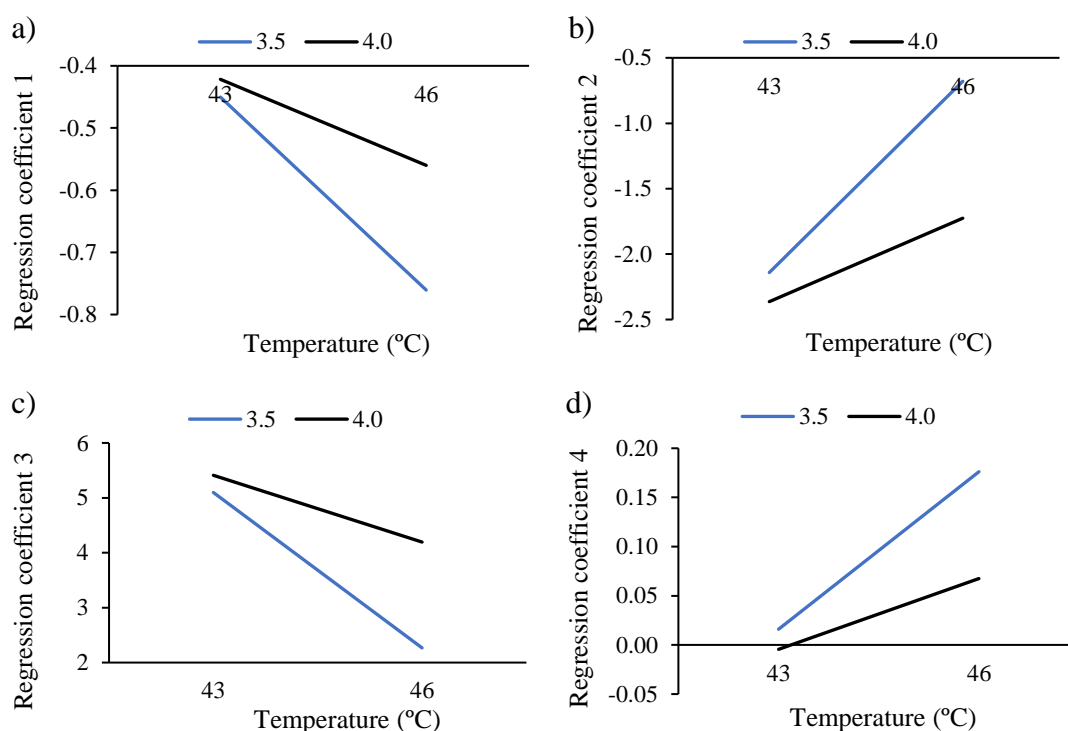


**Fig.11.** Effect of interaction of incubation temperature and protein concentration on the calibration coefficients (1, 2, 3, 4) of the pH prediction model, with adjusted initial voltage gain. Data were means of three replications.

### 3.3 Results of the external pH model with voltage gain adjustment ( $pH_E$ ).

It should be noted that the pH values obtained by this method were discontinuous, and the light backscatter ratio (R) used was acquired from vat #1 of CoAguLab equipment, as its performance was clearly better.

#### 3.3.1 Calibration and validation

Following the same procedure discussed in sections 3.1.1 and 3.2.1, the average values of the three replications obtained at different temperature and protein concentration were shown in Table 4.

**Table 4.** Model performance indicators obtained at different temperature and protein concentration levels (external pH electrode).

Treatments		A		B		C		D		Average $\pm$ SD
Parameters		T (°C)	P (%)	T (°C)	P (%)	T (°C)	P (%)	T (°C)	P (%)	
		43	3.5	43	4.0	46	3.5	46	4.0	
Calibration	$R^2_c$	0.993 $\pm$ 0.004		0.975 $\pm$ 0.018		0.878 $\pm$ 0.087		0.862 $\pm$ 0.088		0.927 $\pm$ 0.049
	SEP <sub>c</sub>	0.015 $\pm$ 0.005		0.026 $\pm$ 0.012		0.050 $\pm$ 0.021		0.053 $\pm$ 0.015		0.036 $\pm$ 0.013
	CV <sub>c</sub>	0.302 $\pm$ 0.096		0.526 $\pm$ 0.250		1.014 $\pm$ 0.435		0.973 $\pm$ 0.012		0.731 $\pm$ 0.271
Validation	$R^2_v$	0.994 $\pm$ 0.003		0.973 $\pm$ 0.012		0.750 $\pm$ 0.323		0.788 $\pm$ 0.137		0.876 $\pm$ 0.119
	SEP <sub>v</sub>	0.022 $\pm$ 0.010		0.049 $\pm$ 0.025		0.081 $\pm$ 0.035		0.102 $\pm$ 0.056		0.064 $\pm$ 0.031
	CV <sub>v</sub>	0.459 $\pm$ 0.200		1.009 $\pm$ 0.515		1.632 $\pm$ 0.682		2.093 $\pm$ 1.176		1.298 $\pm$ 0.643

For treatment combinations A, B, C and D, data were means  $\pm$  standard deviations of three replications.  $R^2_c$ , coefficient of determination of calibration;  $R^2_v$ , coefficient of determination of validation; SEP<sub>c</sub>, standard error of prediction of calibration (pH units); SEP<sub>v</sub>, standard error of prediction of validation (pH units); CV<sub>c</sub>, coefficient of variation of calibration (%); CV<sub>v</sub>, coefficient of variation of validation (%). N, number of experiments, N = 12. N<sub>c</sub>, total number of calibration datapoints, N<sub>c</sub> = 4290. N<sub>v</sub>, total number of validation datapoints, N<sub>v</sub> = 2145.

Although the light backscatter ratio (R) used in this modeling method was the same than that used in section 3.2, there were differences in the pH profiles as they were measured externally, in an attempt to reproduce the current industrial pH determination procedure. It can be observed that the average values of each validation performance indicator obtained for section 3.2 (Table 3) was better than those of Table 4. The effect of temperature and protein on the prediction coefficients was similar to those already discussed in sections 3.1 and 3.2. As in previous cases (vats #1 and #2), the fitting of the established prediction model was optimal under conditions of 3.5% of protein concentration and a fermentation temperature of 43 °C ( $R^2_v = 0.994 \pm 0.003$ , SEP<sub>v</sub> = 0.022  $\pm$  0.010, CV<sub>v</sub> = 0.459  $\pm$  0.200).

The relationship between pH predicted and true values is shown in Fig. 12.

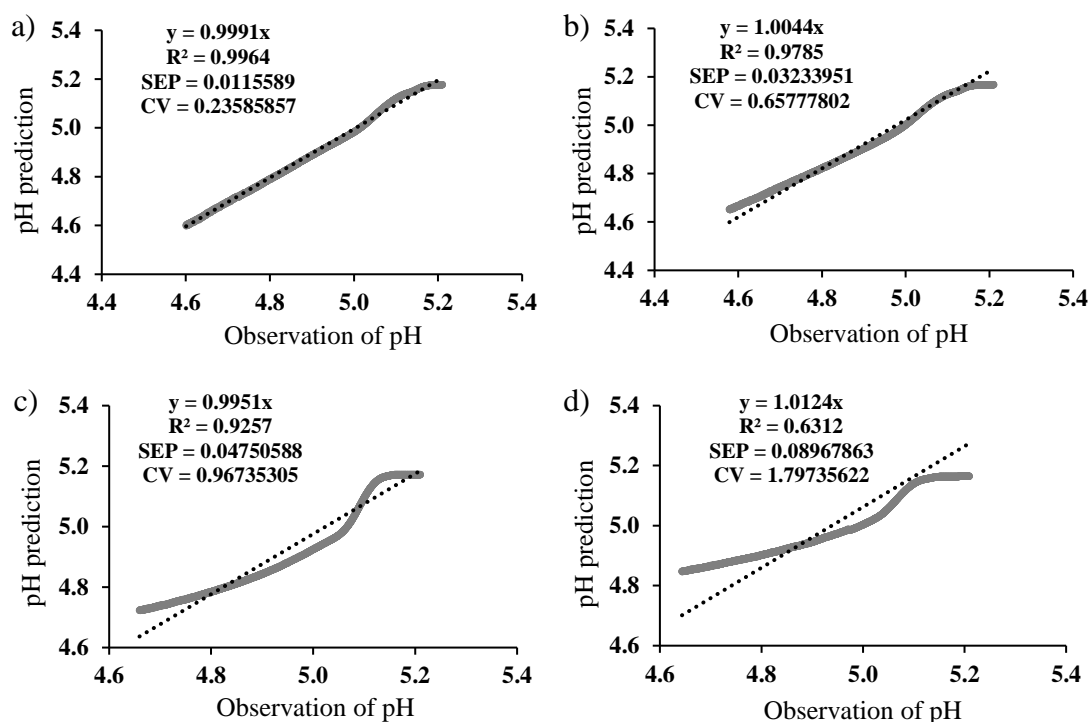


**Fig. 12.** Validation of the pH prediction model, with adjusted initial voltage gain. Validation data corresponding to replication 2; pH data from the external pH electrode. N, number of validation datapoints;  $R^2$ , coefficient of determination; SEP, standard error of prediction (pH units); CV, coefficient of variation (%). a) data at 43 °C and 3.5% of protein. N = 1742; b) data at 43 °C and 4.0% of protein. N = 1857; c) data at 46 °C and 3.5% of protein. N = 2503; d) data at 46 °C and 4.0% of protein. N = 2571.

The results of Figs. 12a and 12b showed that the accuracy of the pH prediction model was optimum at 43 °C, in line with expectation. However, at 46 °C, although the pH predicted values shown in Figs. 12c and 12d were not suitable, predictions were better than those shown in Figs. 5c and 5d corresponding to vat #2 (no voltage gain adjustment) under the same experimental conditions.

### 3.3.2 Effects of temperature, protein and interaction between these two factors on the calibration coefficients

Unlike the above two cases, the factors related to the *Rep* in this model cannot be eliminated. For calibration coefficient 3, *Rep*, *Rep* x T, *Rep* x P were significant ( $p <$

0.05) while for calibration coefficient 4, only *Rep* x *P* was significant ( $p < 0.05$ ).

The influence of the main experimental factors (*T* and *P*) on the calibration regression coefficients were as shown in Figs. 13 and 14.

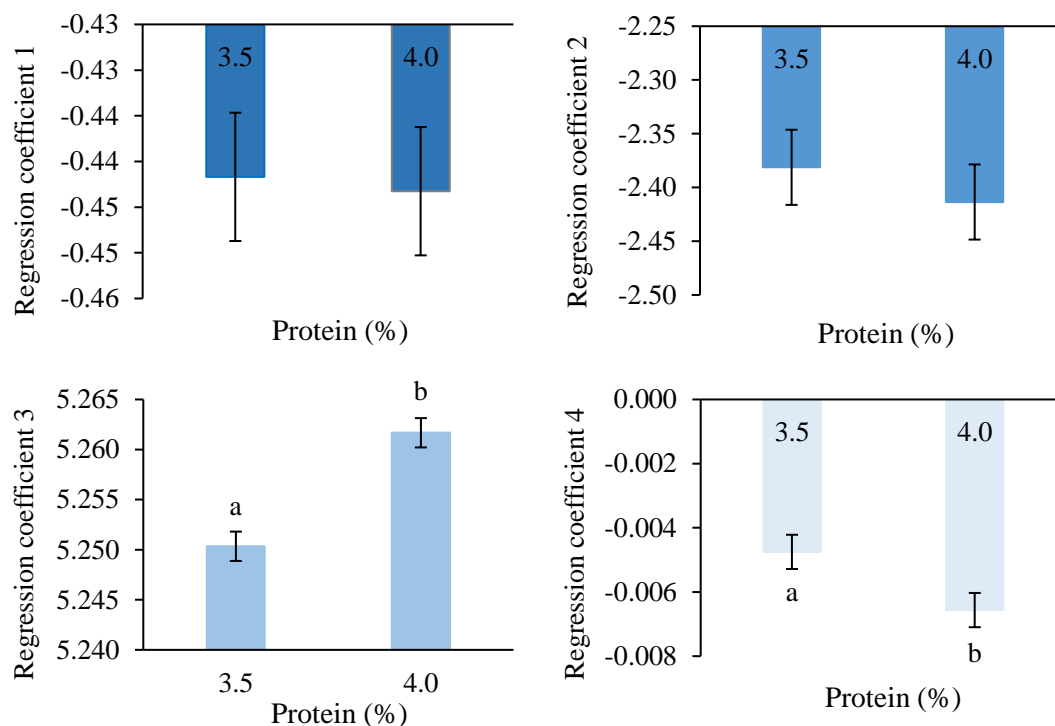


**Fig. 13.** Effect of different protein concentration on the calibration coefficients (1, 2, 3, 4) of the pH prediction model, with adjusted initial voltage gain; data from the external pH measurements. The error bars represented the standard deviation,  $N = 12$ . Least squares means (LSM) with different letters within the same subfigure are significantly different ( $p < 0.05$ ). Least squares means (LSM) without letters indicates no significantly different ( $p \geq 0.05$ ).

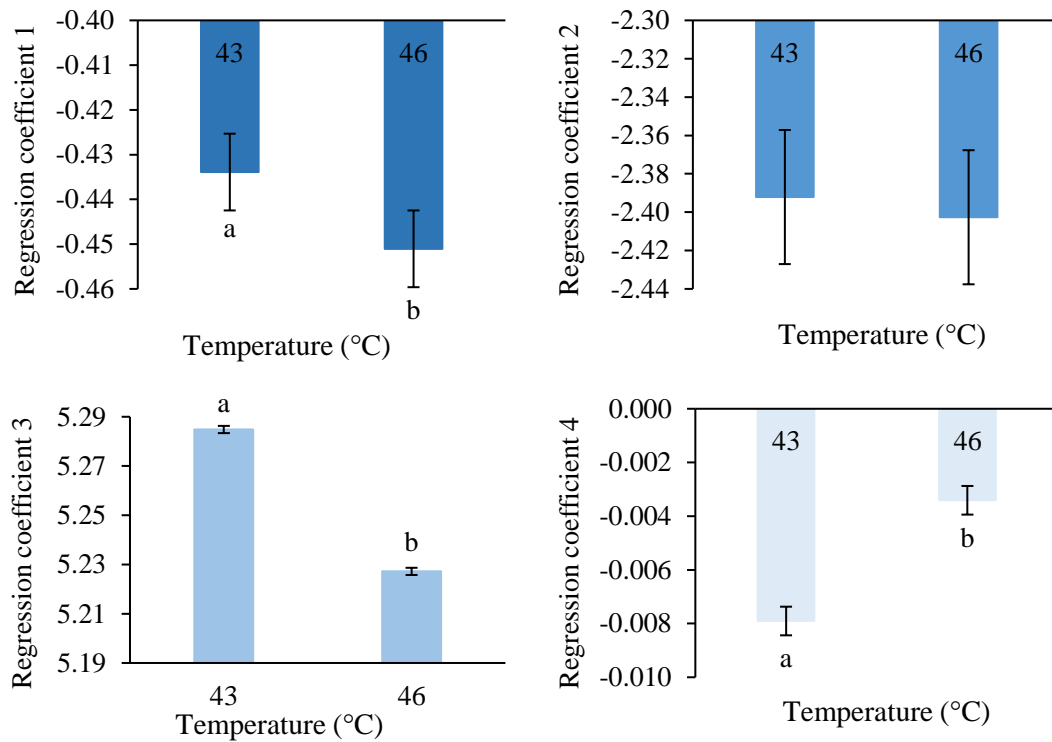


**Fig. 14.** Effect of different incubation temperature of the yogurt fermentation on the calibration coefficients (1, 2, 3, 4) of the pH prediction model, with adjusted initial voltage gain; data from the external pH measurements. The error bars represented the standard deviation, N = 12. Least squares means (LSM) with different letters within the same subfigure are significantly different ( $p < 0.05$ ). Least squares means (LSM) without letters indicates no significantly different ( $p \geq 0.05$ ).

The statistical analysis results of the external pH approach were more complicated. In Fig. 13, the results showed that protein had only a significant effect on calibration coefficients 3, 4, while Fig. 14 showed that the calibration coefficients 1, 3 and 4 were statistically affected by temperature ( $p < 0.05$ ). In summary, the experimental design factors (T, P) were not statistically significant for calibration coefficient 2, which did not affect its results. The calibration factors 3 and 4 were statistically affected by both factors, while for calibration coefficient 1, only temperature affected its results.

In summary, the model validation results corresponding to the continuous pH predictions (vats #1 and #2) and the discontinuous external pH can be summarized as

follows:

1. Irrespectively of the pH acquisition system considered (continuous -*vats #1* and #2-, or discontinuous -*pH<sub>E</sub>*- ), the best fitting of the optical pH prediction model studied was consistently observed with 3.5% protein concentration and 43 °C.
2. The fitting accuracy of the model was greatly affected by temperature. The higher the temperature, the lower the accuracy of the model. This could be attributed to the fact that the prediction model was developed by Arango (2015) at a fermentation temperature of 43 °C. The change in protein concentration had no clear effect on the accuracy of *vat #1* and *pH<sub>E</sub>* predictions; mostly affecting the results of *vat #2* (note that *vat #2* voltage gain was not adjusted).
3. Among the three pH prediction models, the fitting accuracy was ranked from high to low: *vat #1* > *pH<sub>E</sub>* > *vat #2*, which indicated that the initial voltage gain adjusted allowed a better fit of the pH prediction model.
4. Although the model accuracy decreased with increasing temperature, the accuracy observed with 3.5% protein concentration at 43 °C in *vat #2* was worse than that obtained with 3.5% and 4.0% protein concentration at 46 °C in *vat #1*, which clearly confirmed the result of point 3.
5. To monitor the yogurt fermentation process with this model, the pH range was preferably controlled below 5.2. However, since the experimental design factors had only two different levels, the research scope was not wide enough. Additionally, the effect of fat in combination with protein variability was not evaluated. Then, further research is warranted.

## CONCLUSIONS

A NIR light backscatter sensor technology for inline monitoring of yogurt fermentation in combination with a mathematical model to transform the optical signal into real time pH estimations was calibrated and validated at different fermentation temperatures and milk protein concentrations, using three different strategies (continuous pH measurements with and without voltage gain adjustment –*vats #1* and *#2*, respectively– and discontinuous pH readings –*pH<sub>E</sub>*–). Since the optical parameters such as the first maximum of the first NIR light backscatter profile derivative ( $t_{\max}$ ) and the second maximum of the first derivative ( $t_{\max2}$ ) measured by the optical equipment are related to the process of casein micelle aggregation and gel firming, before the calibration and validation of the model, the parameters  $t_{\max}$  and  $t_{\max2}$  were used to preliminarily determine that the effect of temperature on the yogurt fermentation process was greater than that of protein concentration. Further, results of the prediction model performance evaluation showed that the proposed optical and non-destructive method was feasible for inline pH monitoring of industrial yogurt fermentation, compared with the traditional technology, which required manual pH measurement.

The proposed model could determine the endpoint of yogurt fermentation, contributing to better control of the yogurt acidification time. From the experimental results, the model fitted better the experimental pH readings at 43 °C than at 46 °C in the range of pH 5.2–4.6. Among the three calibration strategies evaluated, equipment with initial voltage gain adjustment (*vat #1*) and continuous pH reading was more suitable for this pH prediction model as compared with traditional sampling technology (*pH<sub>E</sub>*) and optical equipment without initial voltage gain adjustment (*vat #2*); however, protein concentration had no significant effect on the results of neither *vat #1* nor *pH<sub>E</sub>* and, even more important, the differences in performance between *vat #1* and *pH<sub>E</sub>* calibration approaches was quite small. In summary, the optical sensor in combination with the prediction model could be used for inline monitoring the yogurt fermentation process, and the highest fitting accuracy was obtained in the equipment with adjusting initial voltages, when set the acidification temperature as 43 °C, a typical yogurt

fermentation temperature.

## REFERENCES

- Arango, O. (2015). Aplicación de dispersión de luz de infrarrojo próximo en la producción de derivados lácteos bajos en grasa con inulina. PhD thesis. UAB, Spain.
- Aswal, P., Shukla A., Priyadarshi S. (2012). Yoghurt: preparation, characteristic and recent advancements. *Cibtech Journal of Bio-Protocols* 1(2): 32-44.
- Cimander, C., Carlsson, M., Mandenius, C.-F. (2002). Sensor fusion for on-line monitoring of yoghurt fermentation. *Journal of Biotechnology*, 99(3), 237–248.
- De Brabandere, A. G., De Baerdemaeker, J. G. (1999). Effects of process conditions on the pH development during yogurt fermentation. *Journal of Food Engineering*, 41(3–4), 221–227.
- Kawasaki, M., Kawamura, S., Tsukahara, M., Morita, S., Komiya, M., Natsuga, M. (2008). Near-infrared spectroscopic sensing system for on-line milk quality assessment in a milking robot. *Computers and Electronics in Agriculture*, 63(1), 22–27.
- Lee, W. J., Lucey, J. A. (2004). Structure and Physical Properties of Yogurt Gels: Effect of Inoculation Rate and Incubation Temperature. *Journal of Dairy Science*, 87(10), 3153–3164.
- Liu, Y. (2010)., *Making method for mung bean yogurt*, China, Patent, No. CN102440284A, 2010-10-13.
- Lucey, J. A., Cheng, T. T., Munro, P. A., Singh, H. (1997a). Rheological properties at small (dynamic) and large (yield) deformations of acid gels made from heated milk. *Journal of Dairy Research*, 64, 591–600.
- Lucey, J. A. (2001). The relationship between rheological parameters and whey separation in milk gels. *Food Hydrocolloids*, 15(4–6), 603–608.
- Lucey, J. A. (2002). Formation and Physical Properties of Milk Protein Gels. *Journal of Dairy Science*, 85(2), 281–294.
- Navrátil, M., Cimander, C., Mandenius, C.F. (2004). On-line multisensor monitoring of yogurt and filmjölkk fermentations on production scale. *Journal of Agricultural And Food Chemistry*, 52(3), 415-420.
- Mellema, M., Walstra, P., Van Opheusden, J. H., Van Vliet, T. (2002). Effects of structural rearrangements on the rheology of rennet-induced casein particle gels. *Advances in Colloid and Interface Science*, 98(1), 25–50.

- Peris, M., Escuder-Gilabert, L. (2013). On-line monitoring of food fermentation processes using electronic noses and electronic tongues: A review. *Analytica Chimica Acta*, 804, 29–36.
- Rasic, J. L., Kurmann, J. A. (1978). *Yoghurt. Scientific grounds, technology, manufacture and preparations*. Technical Dairy Publishing House, Copenhagen.
- Real Decreto-ley 271/2014, de 11 de abril, por el que se aprueba la Norma de Calidad para el yogur o yoghurt. Boletín Oficial del Estado, de 28 de abril de 2014, núm. 102, pp. 33154–33157.
- Soukoulis, C., Panagiotidis, P., Koureli, R., Tzia, C. (2007). Industrial Yogurt Manufacture: Monitoring of Fermentation Process and Improvement of Final Product Quality. *Journal of Dairy Science*, 90(6), 2641–2654.
- Tabayehnejad, N., Castillo, M., Payne, F. A. (2012). Comparison of total milk-clotting activity measurement precision using the Berridge clotting time method and a proposed optical method. *Journal of Food Engineering*, 108(4), 549–556.
- Tamime, A. Y., Robinson, R. K. (2007). *Tamime and Robinson's Yoghurt: Science and Technology* (3rd ed.). Boca Raton: CRC Press.
- Wesstrom, O. (2001). *Inline pH Measurement for the Food/Dairy and Beverage Industry*. Endress & Hauser Inc, Switzerland.
- Yu, F. (2004). 酸奶生产中的关键控制点研究 [Study on the critical control points of yogurt production]. PhD thesis. Nanjing Agricultural University. (in Chinese with English abstract).